HHS Public Access

Author manuscript

Cancer Immunol Res. Author manuscript; available in PMC 2021 January 22.

Published in final edited form as:

Cancer Immunol Res. 2016 June ; 4(6): 531–540. doi:10.1158/2326-6066.CIR-15-0250.

Antibody-Mediated Phosphatidylserine Blockade Enhances the Antitumor Responses to CTLA-4 and PD-1 Antibodies in Melanoma

Bruce D. Freimark[1], **Jian Gong**[1], **Dan Ye**[2], **Michael J. Gray**[1], **Van Nguyen**[1], **Shen Yin**[1], **Michaela M.S. Hatch**[3], **Christopher C.W. Hughes**[3], **Alan J. Schroit**[4], **Jeff T. Hutchins**[1], **Rolf A. Brekken**[2,4], **Xianming Huang**[2]

[1]Department of Preclinical Research, Peregrine Pharmaceuticals, Inc., Tustin, California

[2]Hamon Center for Therapeutic Oncology Research, Departments of Surgery and Pharmacology, UT Southwestern Medical Center, Dallas, Texas

[3]Department of Molecular Biology and Biochemistry, University of California, Irvine, California

[4]Simmons Cancer Center, University of Texas Southwestern Medical Center, Dallas, Texas

Abstract

In tumor-bearing animals, the membrane phospholipid phosphatidylserine (PS) suppresses immune responses, suggesting that PS signaling could counteract the antitumor effect of antibody-driven immune checkpoint blockade. Here, we show that treating melanoma-bearing mice with a PS-targeting antibody enhances the antitumor activity of downstream checkpoint inhibition. Combining PS-targeting antibodies with CTLA-4 or PD-1 blockade resulted in significantly greater inhibition of tumor growth than did single-agent therapy. Moreover, combination therapy enhanced $CD4^+$ and $CD8^+$ tumor-infiltrating lymphocyte numbers; elevated the fraction of cells expressing the proinflammatory cytokines IL2, IFNγ, and TNFα; and increased the ratio of CD8 T cells to myeloid-derived suppressor cells and regulatory T cells in tumors. Similar changes in immune cell profiles were observed in splenocytes. Taken together, these data show that antibody-mediated PS blockade enhances the antitumor efficacy of immune checkpoint inhibition.

Corresponding Author: Xianming Huang, University of Texas Southwestern Medical Center at Dallas, 2201 Inwood Road, NC7304, Dallas, TX 75390-9041. Phone: 214-648-1623; Fax: 214-648-1613; xianming88@yahoo.com.

Authors' Contributions

Conception and design: B.D. Freimark, J. Gong, M.J. Gray, A.J. Schroit, J.T. Hutchins, R.A. Brekken, X. Huang

Development of methodology: B.D. Freimark, J. Gong, V. Nguyen, X. Huang

Acquisition of data (provided animals, acquired and managed patients, provided facilities, etc.): B.D. Freimark, J. Gong, V. Nguyen, S. Yin, M.M.S. Hatch, C.C.W. Hughes, X. Huang

Analysis and interpretation of data (e.g., statistical analysis, biostatistics, computational analysis): B.D. Freimark, J. Gong, M.J. Gray, V. Nguyen, S. Yin, C.C.W. Hughes, A.J. Schroit, R.A. Brekken, X. Huang

Writing, review, and/or revision of the manuscript: B.D. Freimark, J. Gong, C.C.W. Hughes, A.J. Schroit, J.T. Hutchins, R.A. Brekken, X. Huang

Administrative, technical, or material support (i.e., reporting or organizing data, constructing databases): D. Ye, R.A. Brekken Study supervision: B.D. Freimark, J. Gong, J.T. Hutchins, R.A. Brekken, X. Huang

Note: Supplementary data for this article are available at Cancer Immunology Research Online (http://cancerimmunolres.aacrjournals.org/).

Introduction

Cancer immunotherapy is predicated on enhancing the body's natural defenses to control tumor growth by circumventing key processes that drive immune suppression and promote tolerance (1–3). These include soluble mediators, such as IL10 (4) and TGFβ (5), and various cell types, including regulatory T cells (Treg; refs. 6, 7), myeloid-derived suppressor cells (MDSC; ref. 3), and M2-like tumor-associated macrophages (8).

Several therapeutic approaches inhibit T-cell checkpoint mechanisms. These include antibodies that block the activity of CTLA-4 and PD-1 immunoregulatory pathways, which the FDA has recently approved for the treatment of malignant melanoma and lung cancer (9–13). This progress has led to an intense search for agents that block other inhibitory pathways, including indoleamine-2, 3-dioxygenase (IDO; refs. 14, 15), lymphocyte-activation gene 3 (LAG3; refs. 16, 17), and Tim3 (18, 19) and for agonists that activate immune stimulatory pathways, such as 4–1BB (CD-137; refs. 20, 21), OX40 (22, 23), inducible T-cell costimulator (24), and GITR. Indeed, in preclinical melanoma studies, the combination of multiple immunotherapies (e.g., anti–PD-1 and anti–CTLA-4) has shown significantly better efficacy than single-agent therapy. Unfortunately, a large fraction of melanoma patients remain nonresponsive even when combination therapy is employed (12, 13).

The membrane phospholipid, phosphatidylserine (PS), is an upstream immune checkpoint (25–27). In normal, nontumorigenic cells, PS is localized in the inner leaflet of the plasma membrane but becomes externalized to the outer leaflet of the plasma membrane in cells in the tumor microenvironment because of hypoxia, oxidative stress, cytokine signaling, and cell trafficking (25, 28). Externalized PS is also a well-characterized cell marker that is primarily responsible for the recognition and uptake of dying apoptotic cells by phagocytes and for quelling potential autoimmune responses (28). Activation of phagocytic cells is mediated by the interaction of PS with the TAM (TYRO3, AXL, and MERTK) and TIM (T-cell immunoglobulin and mucin) families of PS receptors that induce expression of immune suppressive cytokines, dampen inflammatory signaling mechanisms, and inhibit innate immune cellular responses (29–31). Tumor vasculature—endothelial cells (32, 33), tumor-derived microvesicles (34), and tumor cells all exhibit PS-mediated "apoptotic mimicry" to suppress proinflammatory antitumor immune responses (35–37). Externalization of PS also dampens the adaptive immune response. When intratumoral dendritic cells bind and ingest PS-expressing cells, they maintain an immature phenotype that prevents the expression of costimulatory molecules required for functional antigen presentation (26, 38). Moreover, PS externalized on tumor-derived microvesicles suppresses activation of T-cell responses (39), and administration of PS-expressing liposomes containing insulin restores tolerance in a murine model of autoimmune diabetes (40). Lastly, although chemotherapy induces tumor cell apoptosis, the concomitant expression of PS on these cells (41, 42) further suppresses potential immune-associated antitumor responses (43).

PS-targeting antibodies that bind with high affinity to PS through β2-glycoprotein 1 (β2GP1) have been developed (33, 41). These antibodies bind indirectly to PS-expressing membranes by cross-linking two molecules of β2GP1 that interact directly with externalized

PS. Preclinical studies have shown that PS-targeting antibodies localize to PS-expressing tumors and tumor endothelial cells and elicit strong antitumor effects when combined with chemotherapy or radiotherapy (33, 41, 42, 44). A PS-targeting antibody, bavituximab, is currently being tested in multiple advanced stage clinical trials for the treatment of solid tumors (45, 46).

In this study, we examined whether a PS-targeting antibody, ch1N11, enhances the antitumor activity of established checkpoint inhibitors in mouse melanoma. Our data show that combination therapy with ch1N11 and downstream immune checkpoint blockade induces more $CD8^+$ T cells and fewer immune suppressive MDSCs and M2 macrophages, resulting in potent antitumor efficacy.

Materials and Methods

Cell lines

Mouse melanoma K1735 (47) was obtained in 2010 from the laboratory of Dr. Isaiah Fidler, The University of Texas MD Anderson Cancer Center (Houston, TX). B16F10 was obtained from the ATCC (CRL-6475) in 2013. B16F10 and K1735 cells are of mouse origin and were not authenticated before use. Cells were maintained in RPMI-1640 (GIBCO) supplemented with 10% heat-inactivated FBS (GIBCO) and cultured for approximately 3 weeks before use. Cells were confirmed to be free of *Mycoplasma* before use.

Antibodies

PS-targeting antibody chimeric 1N11 (ch1N11) is a mouse IgG2a-κ with human variable heavy and light chain regions, which binds PS in the presence of both mouse and human beta-2 glycoprotein 1 (Supplementary Fig. S1). C44, a mouse IgG2a isotype control, and hybridoma cell line producing UC10–4F10–11, a mAb to mouse CTLA-4, were obtained from the ATCC. Purified mAb to mouse PD-1 (clone RMP1-14) was obtained from BioXcell. All antibodies injected in animals tested negative for endotoxin with a limit of detection of 0.05 EU/mL of stock antibody. Specific mAbs to mouse antigens used for fluorescence-activated cell sorting (FACS) analysis were CD3, CD4, CD8a, CD137, Ki-67, granzyme B, FoxP3, IFNγ, TNFα, CD11b, F4/80, GR-1, CD11c, and CD45, and were obtained from BD Pharmingen or E-Bioscience. Additional information on the specific antibodies is provided in Supplementary Table S1.

Animal studies

MaleC3H/He mice and female C57BL/6 mice 6 to 10 weeks old were purchased from Charles River Laboratories. All studies were approved by the Institutional Animal Care and Use Committee at the University of California, Irvine and University of Texas Southwestern Medical Center. K1735 tumor cells were suspended at 10^7/mL, and B16F/10 tumor cells were suspended at 2×10^6/mL in 50% (v/v) Matrigel in PBS and 0.1 mL was injected s.c. into the right flank. Tumor volumes (V) were calculated using the formula $V = L \times W^2/2$, were L is the largest and W is the smallest diameter of the tumor. Percent tumor growth inhibition (%TGI) was calculated using the formula $\%TGI = 1 - (T/C) \times 100$, where T = mean tumor volume of treated group at the end of study, C = mean tumor volume of control

group at the end of study. Antibodies were administered i.p. in phosphate-buffered saline once or twice per week at 5 to 10 mg/kg as indicated.

Flow cytometry

K1735 tumors were excised from mice when volumes of approximately 800 to 1,000 mm^3 were achieved. B16F10 tumors were excised from mice on day 12 after implantation. The tumors were minced and digested with a cocktail containing collagenase (1 mg/mL; Sigma), hyaluronidase (0.1 mg/mL; Sigma), and DNase type IV (200 units/mL; Sigma) for 2 hours at 20°C and passed through a 70-μm sieve (Falcon). The cell suspensions were washed twice with PBS and stained with the indicated antibodies for 20 minutes at 4°C. Intracellular staining of cytokines in tumor-infiltrating T cells (TIL) was determined by culturing tumor suspensions in complete medium for 5 hours with ionomycin (500 ng/mL; Sigma Aldrich), phorbol myristate acetate (5 ng/mL; Sigma Aldrich), and Golgi Plug (BD Biosciences) at 3 μg/mL. Surface-stained cells were fixed, permeabilized, and stained using a kit for intracellular cytokines (BD Biosciences) and for FoxP3 (eBioscience) according to the manufacturer's instructions. Cells were analyzed using a FACS Verse flow cytometer (Becton Dickenson), and analysis was performed using Flow Jo v10.0.8 (FlowJo, LLC).

Immunohistochemistry

Tumors were embedded in optimal cutting temperature medium, frozen in a dry-ice isopentane bath, and sectioned through the largest radius. Tissue sections (5 mm) were stained for the following cell types: Total immune cells (CD45), T cells (CD3, CD4, and CD8), TAMs (F4/80), M1-type TAMs (iNOS and F4/80), M2-type TAMs (Arg-1 and F4/80), MDSCs (CD11b and Gr-1), and Tregs (CD4 and FoxP3). Additional information on specific antibodies is provided in Supplementary Table S1. The sections were stained with peroxidase- or alkaline phosphatase–labeled secondary antibodies and counterstained with hematoxylin and analyzed by bright-field microscopy. Slides were digitized using an Aperio ScanScope XT Image System, and immunostained cells were quantified using Aperio Imagescope software. Specific staining was determined by calculating the number of pixels showing positive immunostaining in each tumor less the intensity of an isotype control. Necrotic regions were excluded.

IFNγ ELISpot

Splenocytes from antibody-treated B16-bearing mice were harvested 12 days after tumor implantation. Single-cell splenocyte preparations were resuspended in RPM1–1640 supplemented with 10% FCS, and antibiotics at 10^6 cells/mL and 100 μL aliquots were added, in triplicate, to wells of ELISpot microplates coated with anti-mouse IFNγ Ig. Plates were incubated for 48 hours at 37°C, and spots were developed with anti-mouse IFNγ IgG–HRP conjugate followed by peroxidase substrate. Spots were counted using an automated ELISpot plate reader.

Statistical analysis

Statistical analyses were conducted using Graph Pad Prism version 6 for Windows (GraphPad Software). Statistically significant differences between treatment groups were

determined by the Student *t* test. Values of $P < 0.05$ were considered statistically significant. Asterisks on graphs denote the level of statistical significance for $P < 0.05$ (*), $P < 0.01$ (**), $P < 0.005$ (***), and $P < 0.001$ (****).

Results

PS targeting enhances the efficacy of checkpoint blockade

Single-agent treatment of murine melanomas with inhibitors of the CTLA-4 or PD-1 pathways has been shown to inhibit tumor growth; however, combinatorial therapy that inhibits multiple immune checkpoints results in significantly improved efficacy (1, 48). We found that antibody-mediated blockade of PS signaling enhanced the efficacy of anti–CTLA-4 and anti–PD-1 antibodies in two murine melanoma models. Treatment of animals with K1735 tumors with ch1N11 inhibited tumor growth by 29% compared with control IgG (Fig. 1A). Combination of ch1N11 and anti–CTLA-4 antibody inhibited tumor growth by 68% compared with 13% using anti–CTLA-4 treatment alone (Fig. 1A), whereas combination of ch1N11 and PD-1–blocking antibodies inhibited tumor growth by 87% compared with 69% for anti–PD-1 treatment alone (Fig. 1B). Similar results were obtained with a second melanoma line. The treatment of animals bearing B16 tumors with ch1N11 inhibited tumor growth by 40% to 58% compared with control IgG (Fig. 1C and D). Treatment of mice bearing B16 tumors with a combination of ch1N11 and CTLA-4 blockade inhibited tumor growth by 72%, compared with 47% using anti–CTLA-4 alone (Fig. 1C), whereas combination of ch1N11 and PD-1–blocking antibodies inhibited tumor growth by 65%, compared with 42% using anti–PD-1 treatment alone (Fig. 1D). These results suggest that inhibition of an upstream PS-mediated immune suppressive signaling pathway significantly enhances the therapeutic efficacy of downstream immune checkpoint inhibition ($P < 0.05$).

PS blockade increases immune cell infiltration

The elevated antitumor responses induced by ch1N11 in combination with anti–PD-1 in mice bearing B16 and K1735 tumors suggest that therapy might have induced a phenotypic change of TILs in the tumor microenvironment. In the B16 model, the combination of ch1N11 and anti–PD-1 increased the frequency of $CD45^+$ TILs compared with either ch1N11 or anti–PD-1 alone (Fig. 2A). A statistically significant increase in $CD8^+$ TILs was observed in animals treated with anti–PD-1 as a single agent, or in combination with ch1N11 (Fig. 2B). Moreover, a statistically significant difference was observed in the TIL $CD8^+$/Treg ($CD4^+FoxP3^+$) ratio in animals treated with a combination of ch1N11 and anti–PD-1 compared with anti–PD-1 alone (Fig. 2D). No statistical difference in the TIL $CD4^+$/Treg ($CD4^+FoxP3^+$) ratio was observed among the different treatment groups (Fig. 2C). In the K1735 model, animals treated with ch1N11 and anti–PD-1 had more $CD45^+$ ($P < 0.05$) and $CD8^+$ T cells ($P < 0.005$; Fig. 2E and F; Supplementary Fig. S2) compared with anti–PD-1 alone or control-treated mice. These changes correlated with an increase in the $CD4^+$/Treg ratio ($P < 0.0001$) and $CD8^+$/Treg ratio ($P < 0.01$; Fig. 2G and H).

Combination therapy increases TIL activation and enhances TIL effector function

TILs are often characterized as exhausted by their lack of proliferation, limited production of IL2, IFNγ, and TNFα in response to stimuli, and loss of cytolytic function. To determine whether the therapeutic effect of antibody-mediated PS blockade combined with PD-1 inhibition was a result of reactivation of tumor-infiltrating $CD8^+$ T cells, we utilized an *ex vivo* stimulation protocol designed to favor analysis of preactivated T cells. Responsiveness was assessed by measuring cytokine production by FACS (Fig. 3). In the B16 model, a statistically significant increase in $CD4^+$ $IFN\gamma^+$ cells was observed in TILs from animals treated with the combination of ch1N11 and anti–PD-1 compared with control antibody therapy. TILs from anti–PD-1 and combination-treated animals had similar numbers of $CD8^+$ $IFN\gamma^+$ cells, but more than control-treated animals. Both $CD4^+$ and $CD8^+$ cells that secreted TNFα had similar TIL frequencies in anti–PD-1 and combination-treated animals, but both treatments yielded more of these cells than control-treated animals. In the K1735 model, the frequency of $CD4^+$ and $CD8^+$ TILs producing IFNγ was higher in animals treated with the combination o ch1N11 and anti–PD-1 compared with single agent and control-treated animals. Similarly, the number of $CD4^+$ and $CD8^+$ TILs producing TNFα was higher in animals treated with combination therapy, compared with single-agent therapy. In addition, the frequency of intracellular IL2-producing $CD4^+$TILs was higher after combination therapy, compared with animals treated with either single agent alone. In the K1735 model, granzyme B and Ki67 expression were used as a measure of $CD8^+$ T-cell tumor-killing potential and cell activation (Fig. 4). Animals treated with ch1N11 and anti–PD-1 had more Ki67 (Fig. 4A) and granzyme B (Fig. 4B) in their $CD8^+$ TILs than those from animals treated with single-agent therapy. In addition, the increase in the numbers of $CD4^+CD137^+$ (Fig. 4C) and $CD11b^+$ $iNOS^+$ cells (Fig. 4D) was greater in combination-treated animals compared with animals given single-agent therapy. These data suggest that blockade of PS signaling in combination with PD-1 checkpoint inhibition induces polyfunctional activation of tumor-infiltrating $CD8^+$ T cells.

Increased cytokines in splenocytes after PS blockade

To determine whether blockade of PS combined with inhibition of downstream immune checkpoints enhanced a systemic tumor-specific immune response, we evaluated the number of cytokine-producing splenocytes by FACS and Elispot (Fig. 5). In the K1735 model, the number of $IFN\gamma^+$-producing $CD8^+$ cells was higher in animals treated with ch1N11 and anti–PD-1 compared with control and single treatment groups. In addition, the number of TNFα-secreting $CD4^+$ cells was higher in animals treated with ch1N11 and anti–PD-1 alone and in combination compared with control-treated animals. In the B16 model, splenocytes from animals dosed with a combination of ch1N11 and anti–PD-1 had the highest number of IFNγ Elispots (109 ± 25), which was significtantly higher than anti–CTLA-4 (29.4 ± 4, $P < 0.005$), ch1N11 (16.6 ± 3.2, $P < 0.001$), anti–PD-1 (41.6 ± 5.5, $P < 0.001$), and ch1N11 + anti–CTLA-4 (73.6 ± 13.9, $P < 0.05$) groups; the effectiveness of combined ch1N11 and anti–CTLA-4 was significantly higher than ati–CTLA-4n alone (73.6 ± 13.9 vs. 29.4 ± 4.2, $P < 0.01$), indicating that there were significantly more functional T cells in the spleens of combination-treated groups. In addition, combination treatment slightly increased the frequency of IFNγ-producing splenocytes in naïve tumor-free mice; however, the frequency

was significantly higher in tumor-bearing mice than that of tumor-free mice, indicating tumor-specific T-cell immunity (Supplementary Fig. S3).

Reduction in MDSCs and Tregs after PS blockade

To determine if the enhanced numbers of activated TILs and splenocytes by ch1N11 correlated with a reduction in cells with immunosuppressive phenotypes, spleens and tumors from treated animals were analyzed for MDSCs ($CD11b^+$ $GR\text{-}1^+$) and Tregs ($CD4^+$ $FoxP3^+$) by FACS (Fig. 6). A reduction in the frequency of tumor-associated $CD11b^+$ $GR\text{-}1^+$ cells (Fig. 6A, $P < 0.05$) and $CD11b^+$ $Arg\text{-}1^+$ cells (Fig. 6B, $P < 0.05$) was observed in K1735 tumors following treatment with ch1N11 and anti–PD-1 antibodies compared with control and anti–PD-1 antibody alone (see also Supplementary Fig. S2). A reduction in $CD11b^+$ $Gr\text{-}1^+$ MDSCs following combination therapy was also observed in splenocytes from mice bearing K1735 tumors compared with those from anti–PD-1-treated animals alone (Fig. 6C, $P < 0.05$). Splenic Tregs were reduced in K1735 tumor-bearing animals treated with combination therapy compared with control animals (Fig. 6D, $P < 0.01$). In B16 tumors, no difference in the percentage of tumor Tregs or MDSC was observed in the treatment groups (Fig. 6E and F). Overall, these data suggest that blockade of PS signaling in combination with PD-1 checkpoint inhibition reduces these suppressive cell phenotypes in the tumor and spleen, resulting in enhanced antitumor responses and tumor regression.

Discussion

An underlying challenge to virtually all cytotoxic cancer therapies is therapy-induced exposure of PS that exacerbates immunosuppression in the tumor microenvironment (38, 49, 50). We have found that PS-driven immune suppression can be inhibited by antibody-mediated PS blockade (38, 51). In the present study, we demonstrate that inhibition of upstream PS-mediated immune suppression enhances the efficacy of downstream checkpoint blockade in two murine melanoma models. Blockade of PS combined with anti–CTLA-4 or anti–PD-1 improved tumor control and antitumor immune activation as determined by multiple parameters, including the following: (i) an increase in the activated $CD4^+$ and $CD8^+$ TILs and peripheral immune cells; (ii) a reduction in immunosuppressive intratumoral and peripheral MDSCs and Tregs; and (iii) induction of proinflammatory cytokines IL2, IFNγ, and TNFα from tumor-reactive immune cells. These data are consistent with results from prior studies that found antibody-mediated PS blockade dramatically increased the ratio of M1:M2 macrophages and increased the number of mature dendritic cells in tumors while reducing MDSCs (51). In this study, we have evaluated the effect of PS-targeting antibodies in combination with anti–CTLA-4 and anti–PD-1 in two melanoma models with different sensitivities to therapy. B16 tumors are less immunogenic than K1735 tumors, grow rapidly, and are moderate responders to treatment by immune checkpoint inhibitors (52). In contrast, K1735 tumors are more immunogenic than B16, grow more slowly, and are able to better respond to immune checkpoint blockade. In addition, our observations on the numbers of tumor and peripheral MDSCs and Tregs, and sensitivity to reducing these suppressive cell populations in K1735 versus B16 tumors, may further contribute to the relative responsiveness of these tumors to therapy. In summary, blockade of PS signaling in

combination with PD-1 checkpoint inhibition increases the frequency and activation state of $CD8^+$ TILs and enhances the ratio of $CD8^+$ cells to immunosuppressive MDSCs and Tregs.

The sustained antitumor effect of passive antibody treatment is mediated by specific targeting and/or blocking of suppressive ligands and the interaction of Fc-receptors on myeloid effector cells. Data from previous studies indicate that the Fc portion of PS-targeting antibodies contributes to differentiation of mature dendritic cells because the $F(ab')_2$ fragment alone has lower potential to differentiate splenic monocytic MDSCs from macrophages and dendritic cells (51). Studies show that antibodies to CD20 ligate FcγRIIA receptors on $CD11c^+$ dendritic cells generate a vaccinal effect by stimulating long-term cellular immune responses (53). Thus, the induction of IFNγ secretion from TILs and peripheral immune cells of tumor-bearing animals treated with ch1N11 and anti–PD-1 antibodies may be due to cross-presentation of tumor antigens via Fc receptors on dendritic cells or macrophages. The combination of ch1N11 and anti–CTLA-4 or anti–PD-1 in the B16 tumor model significantly increased the frequency of IFNγ-producing splenocytes compared with single-agent therapy. In contrast, few IFNγ-producing splenocytes were observed from naïve tumor-free animals dosed with the same antibody combinations, suggesting that tumor antigens were required for stimulation (see Supplementary Fig. S3). The activated immune response bias after PS therapy is likely the result of several mechanisms, including the following: (i) opsonization of tumor-derived, PS-expressing microvesicles or cell fragments and subsequent activation of Fc receptors on splenic macrophages; (ii) blockade of immunosuppressive signaling mediated by TIM (especially TIM-3) and TAM PS receptors on immune cells; and (iii) enhanced cross-presentation of tumor antigens by mature dendritic cells due to proinflammatory cytokine upregulation of MHC class II and costimulatory molecules CD80 and CD86.

In summary, we have shown that PS-targeting anti improve the efficacy of anti–CTLA-4 or anti–PD-1 therapy in murine models of melanoma, suggesting that these combinations have the potential to improve outcome in patients with advanced-stage melanoma. Bavituximab, a chimeric PS-targeting antibody, is currently being evaluated in late-stage clinical trials for the treatment of cancer patients with solid tumors (46, 54), and strong antitumor activity has been demonstrated in melanoma clinical trials using checkpoint inhibitor antibodies targeting CTLA-4 (10), PD-1 (12, 13), and PD-L1 (55). It is increasingly apparent that successful immunotherapy requires tumor cell killing, induction of proinflammatory immune responses, and concomitant reduction of immunosuppressive signals leading to increased tumor infiltration by activated T cells. Based on the distinct mechanism of action and multiple points of blockade, PS-targeting antibodies such as bavituximab may enhance the antitumor responses of immune checkpoint inhibitors by further blocking suppressive signals in the tumor microenvironment.

Supplementary Material

Refer to Web version on PubMed Central for supplementary material.

Acknowledgments

The authors thank Jason Toombs and Janie Iglehart for technical assistance.

Grant Support

This work was supported in part by a sponsored research agreement from Peregrine Pharmaceuticals Inc. (to R.A. Brekken).

The costs of publication of this article were defrayed in part by the payment of page charges. This article must therefore be hereby marked advertisement in accordance with 18 U.S.C. Section 1734 solely to indicate this fact.

Disclosure of Potential Conflicts of Interest C.C.W. Hughes is consultant at, and is a consultant/advisory board member for, Peregrine Pharmaceuticals. R.A. Brekken reports receiving commercial research support, has ownership interest (including patents), and is a consultant/advisory board member for Peregrine Pharmaceuticals. X. Huang reports receiving commercial research support from Peregrine Pharmaceuticals, for which he also serves as a consultant/advisory board member. No potential conflicts of interest were disclosed by the other authors.

References

1. Curran MA, Montalvo W, Yagita H, Allison JP. PD-1 and CTLA-4 combination blockade expands infiltrating T cells and reduces regulatory T and myeloid cells within B16 melanoma tumors. Proc Natl Acad Sci U S A 2010;107:4275–80. [PubMed: 20160101]
2. Sakaguchi S, Sakaguchi N, Shimizu J, Yamazaki S, Sakihama T, Itoh M, et al. Immunologic tolerance maintained by CD25+ CD4+ regulatory T cells: Their common role in controlling autoimmunity, tumor immunity, and transplantation tolerance. Immunol Rev 2001;182:18–32. [PubMed: 11722621]
3. Rabinovich GA, Gabrilovich D, Sotomayor EM. Immunosuppressive strategies that are mediated by tumor cells. Annu Rev Immunol 2007; 25:267–96. [PubMed: 17134371]
4. Sharma S, Stolina M, Lin Y, Gardner B, Miller PW, Kronenberg M, et al. T cell-derived IL-10 promotes lung cancer growth by suppressing both T cell and APC function. J Immunol 1999;163:5020–8. [PubMed: 10528207]
5. Chen W, Jin W, Wahl SM. Engagement of cytotoxic T lymphocyte-associated antigen 4 (CTLA-4) induces transforming growth factor beta (TGF-beta) production by murine CD4(+) T cells. J Exp Med 1998;188: 1849–57. [PubMed: 9815262]
6. Shevach EM.CD4+ CD25+ suppressor T cells: More questions than answers. Nat Rev Immunol 2002;2:389–400. [PubMed: 12093005]
7. Sakaguchi S.Naturally arising CD4+ regulatory t cells for immunologic self-tolerance and negative control of immune responses. Annu Rev Immunol 2004;22:531–62. [PubMed: 15032588]
8. Pollard JW. Tumour-educated macrophages promote tumour progression and metastasis. Nat Rev Cancer 2004;4:71–8. [PubMed: 14708027]
9. Wolchok JD, Kluger H, Callahan MK, Postow MA, Rizvi NA, Lesokhin AM, et al. Nivolumab plus ipilimumab in advanced melanoma. N Engl J Med 2013;369:122–33. [PubMed: 23724867]
10. Hodi FS, O'Day SJ, McDermott DF, Weber RW, Sosman JA, Haanen JB, et al. Improved survival with ipilimumab in patients with metastatic melanoma. N Engl J Med 2010;363:711–23. [PubMed: 20525992]
11. Topalian SL, Drake CG, Pardoll DM. Targeting the PD-1/B7-H1(PD-L1) pathway to activate anti-tumor immunity. Curr Opin Immunol 2012;24: 207–12. [PubMed: 22236695]
12. Topalian SL, Hodi FS, Brahmer JR, Gettinger SN, Smith DC, McDermott DF, et al. Safety, activity, and immune correlates of anti-PD-1 antibody in cancer. N Engl J Med 2012;366:2443–54. [PubMed: 22658127]
13. Hamid O, Robert C, Daud A, Hodi FS, Hwu WJ, Kefford R, et al. Safety and tumor responses with lambrolizumab (anti-PD-1) in melanoma. N Engl J Med 2013;369:134–44. [PubMed: 23724846]
14. Uyttenhove C, Pilotte L, Theate I, Stroobant V, Colau D, Parmentier N, et al. Evidence for a tumoral immune resistance mechanism based on tryptophan degradation by indoleamine 2,3-dioxygenase. Nat Med 2003;9: 1269–74. [PubMed: 14502282]
15. Holmgaard RB, Zamarin D, Munn DH, Wolchok JD, Allison JP. Indoleamine 2,3-dioxygenase is a critical resistance mechanism in antitumor T cell immunotherapy targeting CTLA-4. J Exp Med 2013; 210:1389–402. [PubMed: 23752227]

16. Hemon P, Jean-Louis F, Ramgolam K, Brignone C, Viguier M, Bachelez H, et al. MHC class II engagement by its ligand LAG-3 (CD223) contributes to melanoma resistance to apoptosis. J Immunol 2011;186: 5173–83. [PubMed: 21441454]
17. Goding SR, Wilson KA, Xie Y, Harris KM, Baxi A, Akpinarli A, et al. Restoring immune function of tumor-specific CD4+ T cells during recurrence of melanoma. J Immunol 2013;190:4899–909. [PubMed: 23536636]
18. Fourcade J, Sun Z, Benallaoua M, Guillaume P, Luescher IF, Sander C, et al. Upregulation of Tim-3 and PD-1 expression is associated with tumor antigen-specific CD8+ T cell dysfunction in melanoma patients. J Exp Med 2010;207:2175–86. [PubMed: 20819923]
19. da Silva IP, Gallois A, Jimenez-Baranda S, Khan S, Anderson AC, Kuchroo VK, et al. Reversal of NK-cell exhaustion in advanced melanoma by Tim-3 blockade. Cancer Immunol Res 2014;2:410–22. [PubMed: 24795354]
20. Melero I, Shuford WW, Newby SA, Aruffo A, Ledbetter JA, Hellstrom KE, et al. Monoclonal antibodies against the 4-IBB T-cell activation molecule eradicate established tumors. Nat Med 1997;3:682–5. [PubMed: 9176498]
21. Lynch DH.The promise of 4-IBB (CD137)-mediated immunomodulation and the immunotherapy of cancer. Immunol Rev 2008;222: 277–86. [PubMed: 18364008]
22. Kjaergaard J, Tanaka J, Kim JA, Rothchild K, Weinberg A, Shu S. Therapeutic efficacy of OX-40 receptor antibody depends on tumor immunogenicity and anatomic site of tumor growth. Cancer Res 2000; 60:5514–21. [PubMed: 11034096]
23. Curti BD, Kovacsovics-Bankowski M, Morris N, Walker E, Chisholm L, Floyd K, et al. 0X40 is a potent immune-stimulating target in late-stage cancer patients. Cancer Res 2013;73:7189–98. [PubMed: 24177180]
24. Fan X, Quezada SA, Sepulveda MA, Sharma P, Allison JP. Engagement of the ICOS pathway markedly enhances efficacy of CTLA-4 blockade in cancer immunotherapy. J Exp Med 2014;211:715–25. [PubMed: 24687957]
25. Ran S, Thorpe PE. Phosphatidylserine is a marker of tumor vasculature and a potential target for cancer imaging and therapy. Int J Radiat Oncol Biol Phys 2002;54:1479–84. [PubMed: 12459374]
26. Bondanza A, Zimmermann VS, Rovere-Querini P, Turnay J, Dumitriu IE, Stach CM, et al. Inhibition of phosphatidylserine recognition heightens the immunogenicity of irradiated lymphoma cells in vivo. J Exp Med 2004;200:1157–65. [PubMed: 15504819]
27. Kim R, Emi M, Tanabe K. Cancer cell immune escape and tumor progression by exploitation of anti-inflammatory and pro-inflammatory responses. Cancer Biol Ther 2005;4:924–33. [PubMed: 16177562]
28. Balasubramanian K, Schroit AJ. Aminophospholipid asymmetry: A matter of life and death. Annu Rev Physiol 2003;65:701–34. [PubMed: 12471163]
29. Graham DK, DeRyckere D, Davies KD, Earp HS. The TAM family: Phosphatidylserine-sensing receptor tyrosine kinases gone awry in cancer. Nat Rev Cancer 2014;14:769–85. [PubMed: 25568918]
30. Kimani SG, Geng K, Kasikara C, Kumar S, Sriram G, Wu Y, et al. Contribution of defective PS recognition and efferocytosis to chronic inflammation and autoimmunity. Front Immunol 2014;5:566. [PubMed: 25426118]
31. Freeman GJ, Casasnovas JM, Umetsu DT, DeKruyff RH. TIM genes: a family of cell surface phosphatidylserine receptors that regulate innate and adaptive immunity. Immunol Rev 2010;235:172–89. [PubMed: 20536563]
32. Ran S, Downes A, Thorpe PE. Increased exposure of anionic phospholipids on the surface of tumor blood vessels. Cancer Res 2002;62: 6132–40. [PubMed: 12414638]
33. Ran S, He J, Huang X, Soares M, Scothorn D, Thorpe PE. Antitumor effects of a monoclonal antibody that binds anionic phospholipids on the surface of tumor blood vessels in mice. Clin Cancer Res 2005; 11:1551–62. [PubMed: 15746060]
34. Taylor DD, Gercel-Taylor C. Exosomes/microvesicles: mediators of cancer-associated immunosuppressive microenvironments. Semin Immunopathol 2011;33:441–54. [PubMed: 21688197]

35. Fadok VA, Bratton DL, Konowal A, Freed PW, Westcott JY, Henson PM. Macrophages that have ingested apoptotic cells in vitro inhibit proinflammatory cytokine production through autocrine/paracrine mechanisms involving TGF-beta, PGE2, and PAF. J Clin Invest 1998; 101:890–8. [PubMed: 9466984]
36. Fadok VA, Voelker DR, Campbell PA, Cohen JJ, Bratton DL, Henson PM. Exposure of phosphatidylserine on the surface of apoptotic lymphocytes triggers specific recognition and removal by macrophages. J Immunol 1992;148:2207–16. [PubMed: 1545126]
37. McDonald PP, Fadok VA, Bratton D, Henson PM. Transcriptional and translational regulation of inflammatory mediator production by endogenous TGF-beta in macrophages that have ingested apoptotic cells. J Immunol 1999;163:6164–72. [PubMed: 10570307]
38. Cheng AL, Kang YK, Chen Z, Tsao CJ, Qin S, Kim JS, et al. Efficacy and safety of sorafenib in patients in the Asia-Pacific region with advanced hepato-cellular carcinoma: a phase III randomised, double-blind, placebo-controlled trial. Lancet Oncol 2009;10:25–34. [PubMed: 19095497]
39. Kelleher RJ, Balu-Iyer S, Loyall JL, Sacca AJ, Shenoy GN, Peng P, et al. Extracellular vesicles present in human ovarian tumor microenvironments induce a phosphatidylserine dependent arrest in the T cell signaling cascade. Cancer Immunol Res 2015;11:1269–78.
40. Pujol-Autonell I, Serracant-Prat A, Cano-Sarabia M, Ampudia RM, Rodriguez-Fernandez S, Sanchez A, et al. Use of autoantigen-loaded phosphatidylserine-liposomes to arrest autoimmunity in type 1 diabetes. PLoS One 2015;10:e0127057. [PubMed: 26039878]
41. Huang X, Bennett M, Thorpe PE. A monoclonal antibody that binds anionic phospholipids on tumor blood vessels enhances the antitumor effect of docetaxel on human breast tumors in mice. Cancer Res 2005; 65:4408–16. [PubMed: 15899833]
42. He J, Luster TA, Thorpe PE. Radiation-enhanced vascular targeting of human lung cancers in mice with a monoclonal antibody that binds anionic phospholipids. Clin Cancer Res 2007;13:5211–8. [PubMed: 17785577]
43. Kenis H, Reutelingsperger C. Targeting phosphatidylserine in anti-cancer therapy. Curr Pharm Des 2009;15:2719–23. [PubMed: 19689342]
44. Luster TA, He J, Huang X, Maiti SN, Schroit AJ, de Groot PG, et al. Plasma protein beta-2-glycoprotein 1 mediates interaction between the anti-tumor monoclonal antibody 3G4 and anionic phospholipids on endothelial cells. J Biol Chem 2006;281:29863–71. [PubMed: 16905548]
45. Digumarti R, Bapsy PP, Suresh AV, Bhattacharyya GS, Dasappa L, Shan JS, et al. Bavituximab plus paclitaxel and carboplatin for the treatment of advanced non-small-cell lung cancer. Lung Cancer 2014; 86:231–6. [PubMed: 25236982]
46. Gerber DE, Stopeck AT, Wong L, Rosen LS, Thorpe PE, Shan JS, et al. Phase I safety and pharmacokinetic study of bavituximab, a chimeric phosphatidylserine-targeting monoclonal antibody, in patients with advanced solid tumors. Clin Cancer Res 2011;17:6888–96. [PubMed: 21989064]
47. Fidler Ij Fau - Gruys E, Gruys E Fau - Cifone MA, Cifone Ma Fau -Barnes Z, Barnes Z Fau - Bucana C, Bucana C Demonstration of multiple phenotypic diversity in a murine melanoma of recent origin. J Natl Cancer Inst 1981;67:947–56. [PubMed: 6944560]
48. Spranger S, Koblish HK, Horton B, Scherle PA, Newton R, Gajewski TF. Mechanism of tumor rejection with doublets of CTLA-4, PD-1/PD-L1, or IDO blockade involves restored IL-2 production and proliferation of CD8(+) T cells directly within the tumor microenvironment. J Immunother Cancer 2014;2:3. [PubMed: 24829760]
49. Sakuishi K, Apetoh L, Sullivan JM, Blazar BR, Kuchroo VK, Anderson AC. Targeting Tim-3 and PD-1 pathways to reverse T cell exhaustion and restore anti-tumor immunity. J Exp Med 2010;207:2187–94. [PubMed: 20819927]
50. Yan X, Doffek K, Yin C, Krein M, Phillips M, Sugg SL, et al. Annexin-V promotes anti-tumor immunity and inhibits neuroblastoma growth in vivo. Cancer Immunol Immunother 2012;61:1917–27. [PubMed: 22476407]
51. Yin Y, Huang X, Lynn KD, Thorpe PE. Phosphatidylserine-targeting antibody induces M1 macrophage polarization and promotes myeloid-derived suppressor cell differentiation. Cancer Immunol Res 2013;1: 256–68. [PubMed: 24777853]

52. Iwai Y, Terawaki S, Honjo T. PD-1 blockade inhibits hematogenous spread of poorly immunogenic tumor cells by enhanced recruitment of effector T cells. Int Immunol 2005;17: 133–44. [PubMed: 15611321]

53. DiLillo DJ, Ravetch JV. Differential Fc-receptor engagement drives an anti-tumor vaccinal effect. Cell 2015;161:1035–45. [PubMed: 25976835]

54. Digumarti R, Bapsy PP, Suresh AV, Bhattacharyya GS, Dasappa L, Shan JS, et al. Bavituximab plus paclitaxel and carboplatin for the treatment of advanced non-small-cell lung cancer. Lung Cancer 2014;86:231–6. [PubMed: 25236982]

55. Brahmer JR, Tykodi SS, Chow LQ, Hwu WJ, Topalian SL, Hwu P, et al. Safety and activity of anti-PD-L1 antibody in patients with advanced cancer. N Engl J Med 2012;366:2455–65. [PubMed: 22658128]

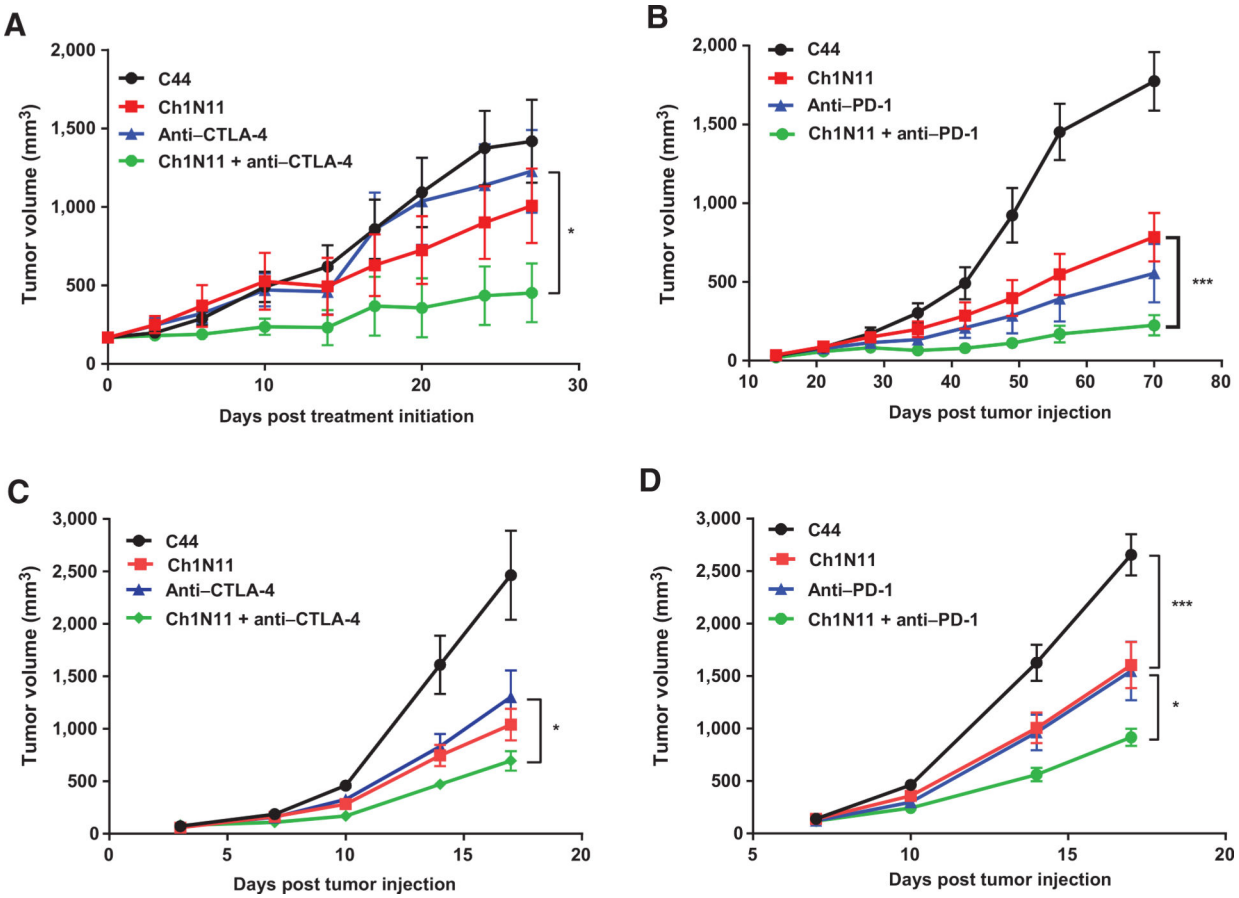

Figure 1.

PS blockade enhances the efficacy of checkpoint inhibition in melanoma tumor models. Mice were inoculated s.c. (day 0) with 1×10^6 K1735 in C3H (A and B) or 1×10^6 B16 in C57BL/6 (C and D), after tumors were established, mice were randomized into groups of 5 to 10 animals per group. Animals were administered i.p. at a dose of 5 mg/kg C44 (isotype control), anti–CTLA-4, anti–PD-1, or ch1N11 in a volume of 200 μL, alone or in combinations as indicated. C3H mice were treated once per week for 4 to 6 weeks. B16 melanoma tumors in C57Bl/6 mice were treated on days 3, 7, and 10. Data are presented as mean ± SEM of 2 to 3 studies of 5 to 10 animals per treatment group. Statistically significant differences between groups were identified by the Student *t* test. *, $P < 0.05$ and ***, $P < 0.005$.

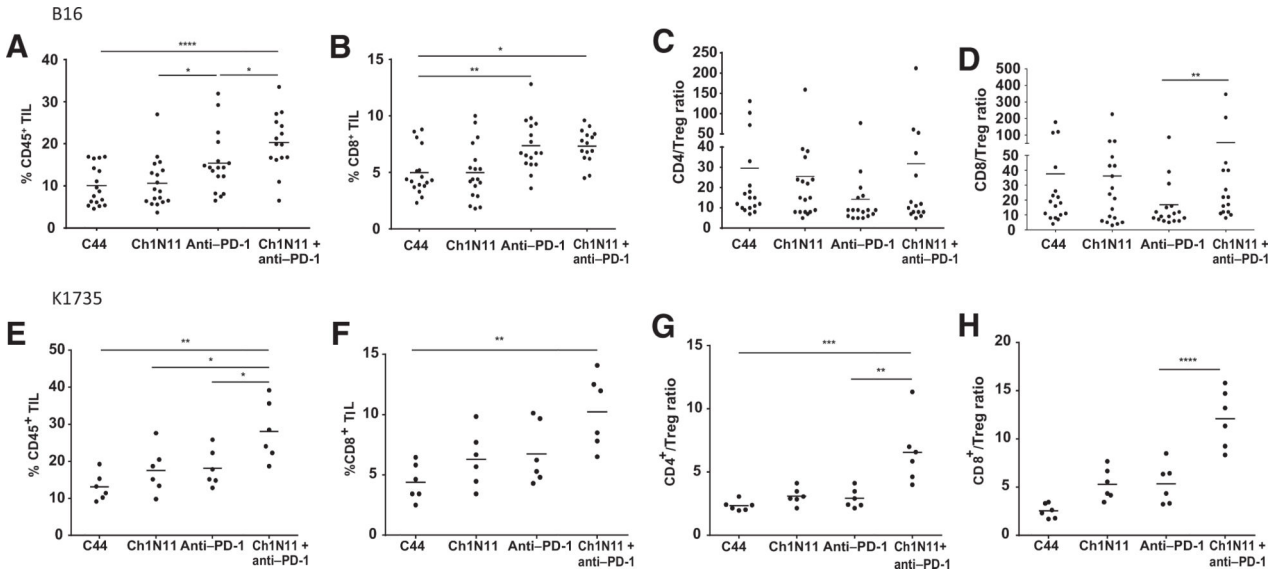

Figure 2.

Immunophenotypic analysis of TILs in B16 and K1735 melanoma following combination therapy with antibodies targeting PS and PD-1. A–D, mice with B16 tumors were treated on days 3, 7, and 10 after tumor implantation with a single antibody or a combination of ch1N11 and anti–PD-1, and tumors were excised on day 12. E–H, K1735 tumors from mice treated weekly with a single antibody or a combination of ch1N11 and anti–PD-1 were excised when tumors reached a size of 800 to 1,000 mm^3. Single-cell preparations of B16 or K1735 tumors were stained with antibodies specific to $CD45^+$ (A and E), $CD8^+$ (B and F), $CD4^+$ Teff/Treg ratio (C and G), and CD8 Teff/Treg ratio (D and H). Data are expressed as group mean and individual animals of %CD45/total cells of dissociated tumor, $\%CD8^+/CD45^+$, $\%CD4^+$/Treg ($CD4^+CD25^+FoxP3^+$), and $\%CD8^+$/Treg by FACS analysis. Statistically significant differences between treatment groups were determined by the Student *t* test. *, $P < 0.05$; **, $P < 0.01$; ***, $P < 0.005$; and ****, $P < 0.001$.

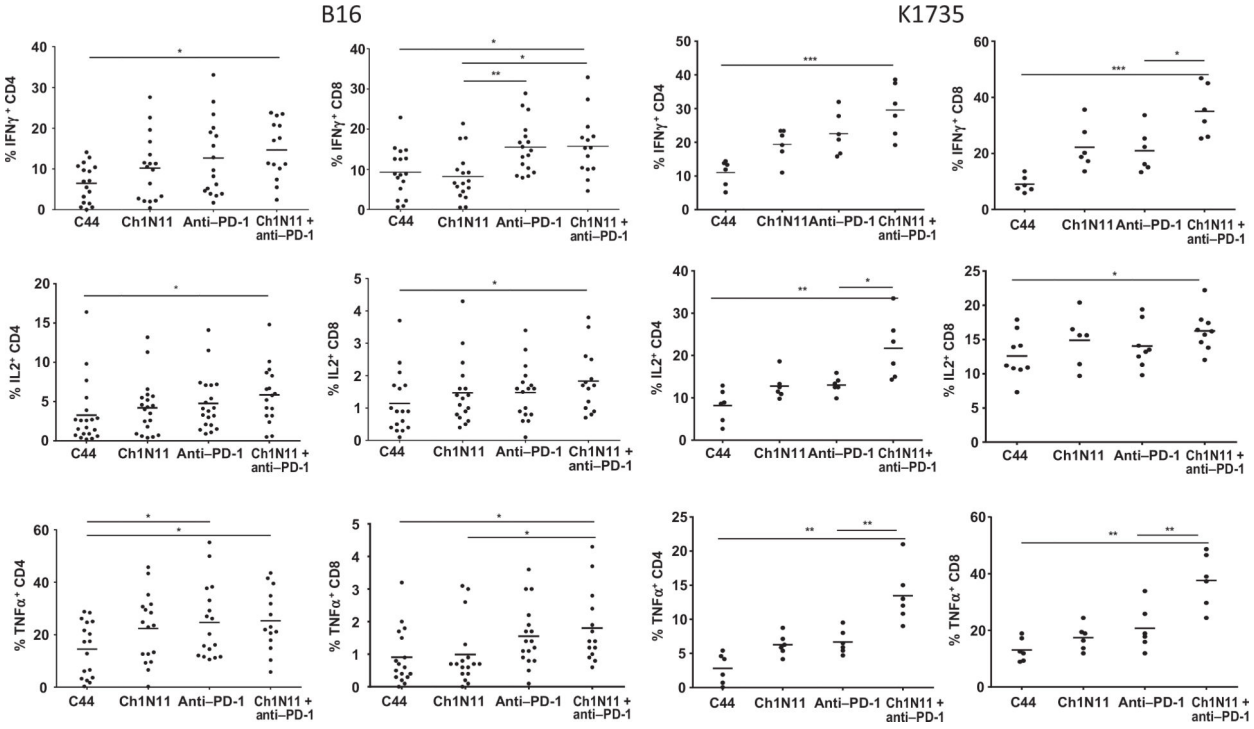

Figure 3.

Cytokine expression in TILs from mice bearing K1735 melanoma following combination therapy with antibodies targeting PS and PD-1. Mice with B16 tumors were treated on days 3, 7, and 10 after tumor implantation with a single antibody or a combination of ch1N11 and anti–PD-1, and tumors were excised on day 12. K1735 tumors from mice treated weekly with a single antibody or a combination of ch1N11 and anti–PD-1 were excised when tumors reached a size of 800 to 1,000 mm^3. Single-cell preparations of tumors were stimulated *in vitro* with PMA and ionomycin for 24 hours and in the presence of brefeldin A for the last 6 hours. Cells were stained for surface CD4, CD8, and CD45 followed by intracellular staining of IFNγ, IL2, and TNFα. Data are expressed as the group mean and individual animal TILs positive for a specific for a surface marker by FACS analysis. Statistically significant differences between treatment groups were determined by the Student *t* test. *, $P < 0.05$; **, $P < 0.01$; and ***, $P < 0.005$.

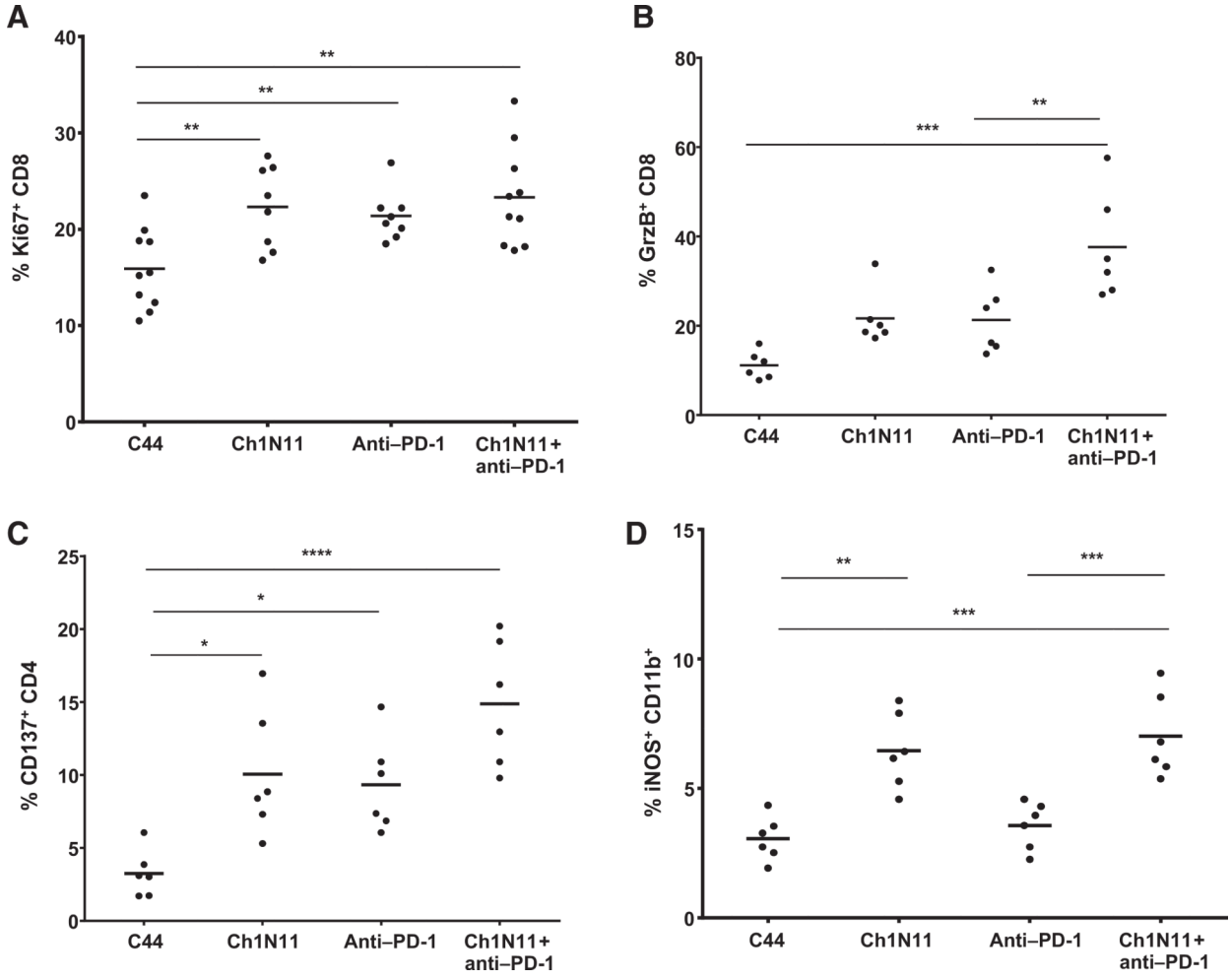

Figure 4.

Activation of TILs in B16 and K1735 melanoma following combination therapy with antibodies targeting PS and PD-1. K1735 tumors from mice treated weekly with a single antibody or a combination of ch1N11 and anti–PD-1 were excised when tumors reached a size of 800 to 1,000 mm^3. TILs were stained for coexpression of CD8 and Ki67 (A), CD8 and granzyme B (B), CD4 and CD137 (C), and CD11b and iNOS (D). Data are expressed as the group mean and individual animal TILs positive for a specific surface marker by FACS analysis. Statistically significant differences between treatment groups were determined by the Student *t* test. *, $P < 0.05$; **, $P < 0.01$; ***, $P < 0.005$; and ****, $P < 0.001$.

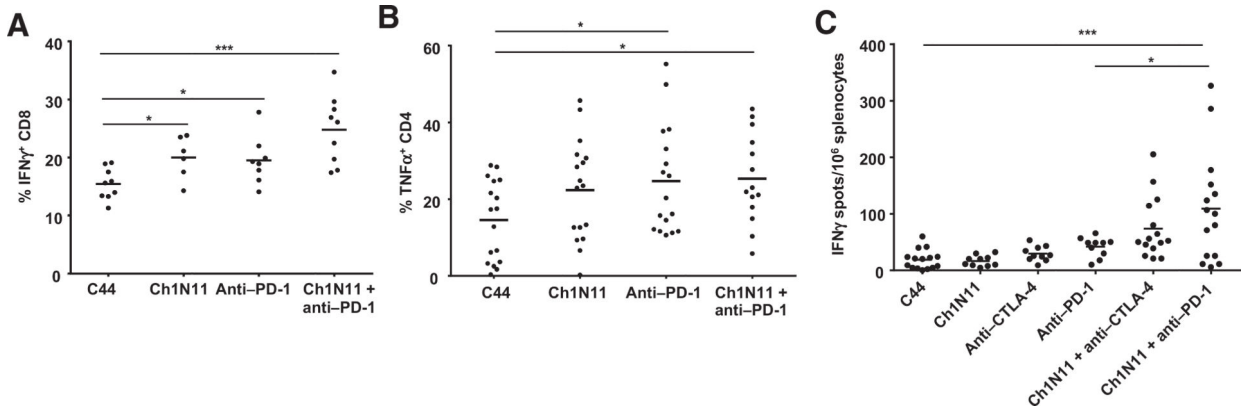

Figure 5.

Cytokine production in splenocytes in B16 and K1735 melanoma following combination therapy with antibodies targeting PS and PD-1. A and B, mice with K1735 tumors were treated weekly with single-agent therapy as indicated, or a combination of ch1N11 and anti–PD-1 and spleens were excised when tumors reached a size of 800 to 1,000 mm^3. Splenocytes from each treatment group were stained for surface CD4, CD8, and CD45 followed by intracellular staining of IFNγ and IL2. C, mice with B16 tumors were treated on days 3, 7, and 10 after tumor implantation with single-agent therapy as indicated or a combination of ch1N11 and anti–PD-1 or anti–CTLA-4, and spleens were excised on day 12. Splenocytes from each treatment group were analyzed for IFNγ secretion by ELISpot. A–C, data are expressed as the group mean and individual animal TILs positive for a specific surface marker by FACS analysis or ELISpot count. Statistically significant differences between treatment groups were determined by the Student *t* test. *, $P < 0.05$ and ***, $P < 0.005$.

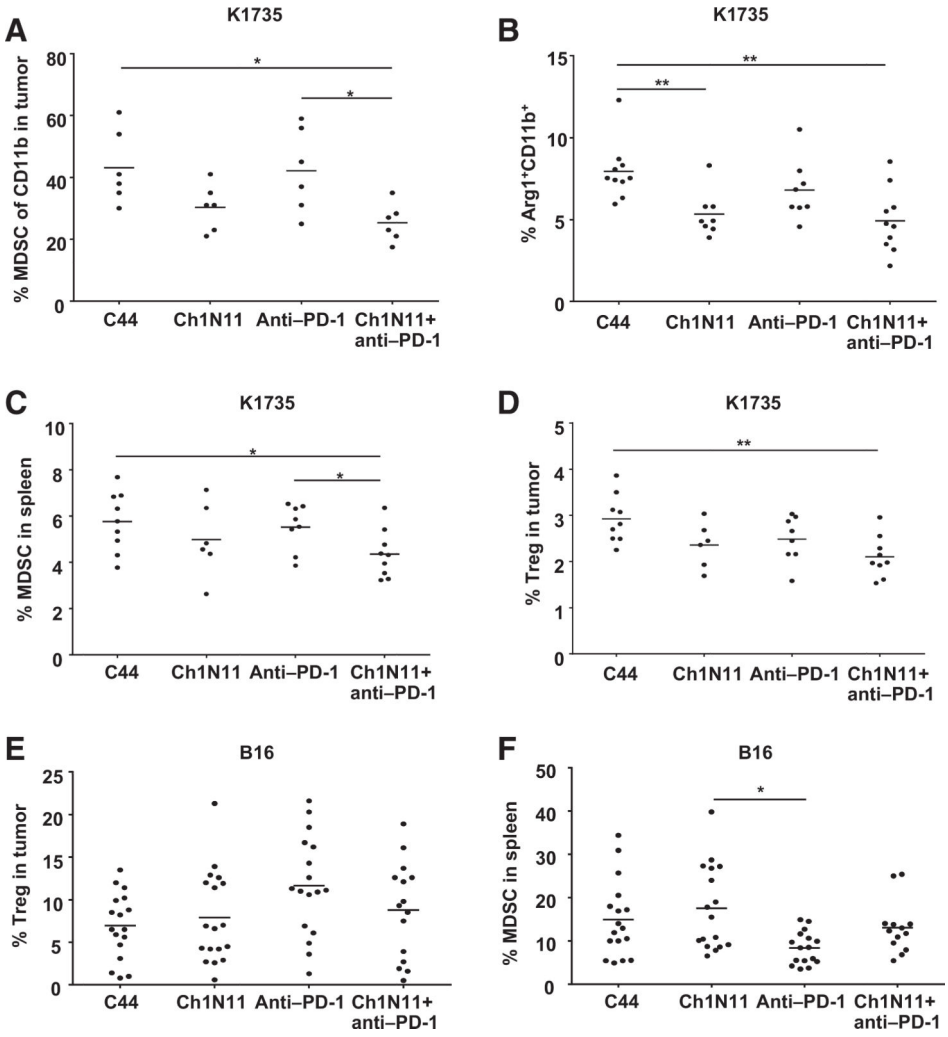

Figure 6.

Reduction in MDSCs and Tregs following combination therapy of antibodies targeting PS and PD-1. Mice with B16 tumors were treated on days 3, 7, and 10 after tumor implantation with a single antibody or a combination of ch1N11 and anti–PD-1 and spleens, and tumors were excised on day 12. K1735 spleens and tumors from mice treated with a single antibody or combinations of antibodies were excised when tumors reached a size of 800 to 1,000 mm^3. Single-cell preparations of tumors were stained with antibodies specific for CD45, MDSC ($CD11b^+$, $GR\text{-}1^+$), Treg ($CD4^+$, $CD25^+$, $FoxP3^+$), and Arg-1. A, summary graph of the percentage of $CD45^+$ $CD11b^+$ in K1735 tumors. B, the percentage of $Arg\text{-}1^+$ $CD11b^+$ in K1735 tumor. C, the percentage of MDSC in spleen in K1735 tumor-bearing mice. D, the percentage of Tregs in spleen of K1735 tumor-bearing mice. E, the percentage of Tregs in B16 tumors. F, the percentage of MDSCs in B16 tumors. Data are presented as results for individual animals and mean per treatment group. Statistically significant differences between treatment groups were determined by the Student *t* test. *, $P < 0.05$ and **, $P < 0.01$.